Received Date : 17-Sep-2013

Revised Date : 26-Mar-2014

Accepted Date : 17-Apr-2014

Article type : Original Articles

The Pan-Caspase Inhibitor Emricasan (IDN-6556) Decreases Liver Injury and Fibrosis in a Murine Model of Non-Alcoholic Steatohepatitis

Fernando J. Barreyro[1, 2];

Holod, Silvia [2];

Finocchietto, Paola V [2];

Camino, Alejandra M [3];

Aquino, Jorge B [4];

Avagnina, Alejandra [5;]

Carreras, María Cecilia [2],

Poderoso, Juan José [2];

Gores, Gregory J [6]

This article has been accepted for publication and undergone full peer review but has not been through the copyediting, typesetting, pagination and proofreading process, which may lead to differences between this version and the Version of Record. Please cite this article as doi: 10.1111/liv.12570

1. Laboratory of Microbiology, Faculty of Chemical and Natural Sciences, National University of Misiones, CONICET (Consejo Nacional de Investigaciones Científicas y Técnicas).

2. Laboratory of Oxygen Metabolism, University Hospital, University of Buenos Aires, Argentina.

3. Laboratorio de Morfometría, DIM Clinica Privada, Buenos Aires, Argentina.

4. Liver Unit, School of Medicine, Austral University, Buenos Aires, Argentina.

5. Department of Pathology, University Hospital, University of Buenos Aires, Argentina.

6. Division of Gastroenterology and Hepatology, Mayo Clinic College of Medicine, Rochester, Minnesota, USA

Address for correspondence:

Fernando Javier Barreyro, MD, PhD

Laboratory of Microbiology, Faculty of Chemical and Natural Sciences, National University of Misiones

1375 Mariano Moreno Avenue

Posadas, Misiones 3300

Tel: 054 376 4435118

Fax: 054 376 4435118

E-mail: fjbarreyro@hospitaldeclinicas.uba.ar

Running title: Emricasan attenuates liver injury in NASH

Key words: Caspase Inhibitor, Emricasan, Apoptosis, Nonalcoholic fatty liver disease, Fibrosis.

Abbreviations: α-SMA, alpha-smooth muscle actin; ALT, alanine aminotransferase; AST, aspartate transaminase; ANOVA, analysis of variance; CHOP, C/EBP homologous protein; CI, confidence interval; CXCL2, C-X-C chemokine ligand-2; HSC, hepatic stellate cell; IL-1β, interleukin 1 beta; HFD, high fat diet; H&E, hematoxylin and eosin; HPF, high-power field; JNK, c-Jun-N-terminal kinase; MCP-1, Monocyte chemoattractant protein; mRNA, messenger RNA; NAFL, nonalcoholic fatty liver; NAFLD, nonalcoholic fatty liver disease; NASH, nonalcoholic steatohepatitis; TG, triglyceride; qPCR, quantitative reverse-transcription polymerase chain reaction; SEM, standard error of the mean; TGF-β, transforming growth factor-β; TIMP-1, tissue inhibitor of metalloproteinase type 1,TNF-α, tumor necrosis factor alpha; TRAIL, tumor necrosis factor–related apoptosis-inducing ligand; TUNEL, terminal deoxynucleotidyl transferase–mediated dUTP nick-end labeling.

SUMMARY

Background: Hepatocyte apoptosis, the hallmark of Non-alcoholic steatohepatitis (NASH) contributes to liver injury and fibrosis. Although, both the intrinsic and extrinsic apoptotic pathways are involved in the pathogenesis of NASH, the final common step of apoptosis is executed by a family of cysteine-proteases termed caspases.

Thus, our aim was to ascertain if administration of Emricasan, a pan-caspase inhibitor, ameliorates liver injury and fibrosis in a murine model of NASH. Methods: C57/BL6J-mice were fed regular chow or high fat diet (HFD) for 20 weeks. All mice were treated with vehicle or Emricasan.

Results: Mice fed a HFD diet demonstrate a 5-fold increase in hepatocyte apoptosis by the TUNEL assay and a 1.5-fold and 1.3-fold increase in caspase-3 and-8 activities respectively; this increase in apoptosis was substantially attenuated in mice fed a HFD treated with Emricasan (HFD-Em). Likewise, liver injury and inflammation were reduced in mice fed HFD-Em as compare to HFD by measuring serum AST and ALT levels, NAS histologic score and IL 1-β, TNF-α, MCP-1 and CXCL2 qPCR. These differences could not be attributed to differences in hepatic steatosis as liver triglycerides content were similar in both HFD groups. Hepatic fibrosis was reduced by Emricasan in HFD animals by decreasing αSMA (a marker for HSC activation), fibrosis score, Sirius red staining, hydroxyproline liver content and profibrogenic cytokines by qPCR.

In Conclusion, these data demonstrate that in a murine model of NASH, liver injury and fibrosis are suppressed by inhibiting hepatocytes apoptosis and suggests that Emricasan may be an attractive anti-fibrotic therapy in NASH

INTRODUCTION

Non-alcoholic fatty liver disease (NAFLD) is currently the most common form of chronic liver disease, affecting 20-30 % of western countries population [1], and is closely associated with insulin resistance (IR) and overweight [2]. A subset of these individuals, approximately 5%, develops hepatic inflammation and fibrosis, a syndrome referral as nonalcoholic steatohepatitis (NASH) [3]. This hepatic inflammatory disorder can progress to cirrhosis, liver failure, and hepatocellular carcinoma [4]. The mechanisms underlying the progression of simple steatosis to steatohepatitis are not known; however, it is recognized that hepatocyte apoptosis correlates with NASH. Indeed, apoptosis is a cardinal pathological feature of NASH and is associated with hepatic inflammation and fibrosis [5]. Consistent with this concept, elevated serum cytokeratin-18 fragments (M30 Neo-epitopes), markers of hepatocyte apoptosis by caspase activation, distinguish simple hepatic steatosis from NASH [6].

Apoptosis, or programmed cell death, is a form of highly regulated cell death. Steatotic hepatocytes can undergo apoptosis via an extrinsic pathway activated by death ligands, Fas [5 7] and tumor necrosis factor related apoptosis inducing ligand (TRAIL) [8 9 10] or via activation of the intrinsic pathway [11 12], which can be triggered by intracellular stress of

membrane-bound organelles, such as lysosomes [13], endoplasmic reticulum (ER) [14], and mitochondria [11]. Both pathways of apoptosis converge on caspases activation which makes this pathway mechanistically attractive by pharmacological inhibition. This group of proteases, term caspases (cysteinyl aspartate specific proteases), play a central role as executors of apoptosis. The caspases are constitutively expressed as inactive proenzymes and generally require proteolytic cleavage on the aspartic acid residue for their activation. Caspases are capable of self activation, as well as of activating each other in a cascade-like process. Among the 14 mammalian caspases identified to date, some are primarily involved in apoptosis (caspases-2, -3, -6, -7, -8, -9, -10, and -12) [15], and other caspases, such as caspases-1, -4, -5, and -11, are involved in inflammation [16]. These caspases can be divided into initiator caspases or effector caspases. Initiator caspases (-2, -8, -9, -10) that are activated by death receptors; and effector caspases (-3, -6, and -7) that require cleavage by initiator caspases for their activation [17]. On initiation of apoptotic cascades, activation of initiator caspases occur causing mitochondria dysfunction, with release of proapoptotic factors into the cytosol (e.g., cytochrome c, SMAC/Diablo, endonuclease G and AIF) [18]. Cytosolic cytochrome c promotes activation of downstream effector caspases, cleavage of cellular targets and dismantle the cell causing characteristic apoptotic morphology. These apoptotic bodies are phagocytosed by adjacent cells, and it has been demonstrated that phagocytosis of apoptotic bodies by Kuppfer cells [19] and hepatic stellate cells (HSC) [20] is one of the mechanisms that promote inflammation and fibrogenesis. Based on this concept, decreasing hepatocytes apoptosis by caspases inhibitors protects the liver in murine models of acute liver failure [21], and attenuates

inflammation and fibrosis in murine models of cholestatic- [22], ethanol- [23] and methionie/choline deficient diet-induced [24 25] liver injury. Thus, the use of a pan-caspase inhibitor could be an attractive therapeutic approach for various types of liver disease. However, its efficacy for long term treatment such as NASH merits further evaluation.

Emricasan (IDN-6556) is an irreversible pan-caspase inhibitor, orally active that is retained in the liver for prolonged period of time [26 21], which was evaluated in clinical trials for chronic liver disease [27 28]. Therefore, in this study, we examined the effect of the pan-caspase inhibitor emricasan on liver injury and fibrosis in a diet induced metabolic syndrome with NASH murine model. To address our aim, we formulated the following questions: Does the pan-caspase inhibitor … 1) attenuate hepatocyte apoptosis and liver injury?, 2) reduce hepatic steatosis?, 3) decrease hepatic inflammation?, and 4) attenuate hepatic fibrogenesis in diet induced NASH model?. The results demonstrate that in a murine model of NASH, liver injury and fibrosis are attenuated by inhibiting hepatocytes apoptosis and suggest that emricasan may be an attractive anti-fibrotic therapy in NASH.

EXPERIMENTAL PROCEDURES

Reagents and diet: Sucrose, Direct red 80 and Fast-green FCF (color index 42053) were obtained from Sigma. Emricasan (formerly named IDN-6556 or PF-03491390), was provided by Pfizer Ltd., was suspended in vehicle [2% (v/v) DMSO in 0.5% (w/v) methylcellulose] and administered to mice per os daily. The high fat diet used was from Cathedra of Bromatology, Faculty of Pharmacy and Biochemistry, University of Buenos

Aires (Cátedra de Bromatología. Facultad de Farmacia y Bioquímica. Universidad de Buenos Aires), which contains 47% of calories from fat (mostly from Milk fat, 50% saturated fat) with 2% of cholesterol, 35% from carbohydrate (78% of carbohydrate from Sucrose) and 18% of calories from protein, and was designed to approximate the typical human diet from patients with NASH [29 30].

Animals. Studies were performed in male C57BL/6J mice (Bioterio Central, Facultad de Ciencias Exactas y Naturales, Universidad de Buenos Aires). All animals were maintained in a temperature (24°C) and light controlled (12:12 hr light:dark) facility, and had free access to food and water. Animals were age-matched and used at approximately 12-16 weeks of age. Four groups were studied (n = 60) with 15 mice per group. Groups 1 and 3 received regular chow. Groups 2 and 4 received high fat diet and 50 g/L (Sucrose) was added to drinking water for 20 weeks. Groups 3 and 4 received Emricasan 0.3mg/kg/day i.g., and group 1 and 2 received the vehicle. The dosing was based on previous data [21] that demonstrates that oral administration of emricasan at doses of 0.3 mg/kg corresponded to the ED90 value to prevent liver injury in the model of α-Fas-induced liver injury. Total body weight was measured at 0, 5, 10, 15 and 20 weeks. All protocols dealing with animals were reviewed and approved by the University of Buenos Aires Animal Studies Committee (CICUAL, Comité Institucional de Cuidado y Uso de Animales de Experimentación). This study followed the guidelines outlined in the National Institutes of Health Guide for the Care and Use of Laboratory Animals.

Serum and Tissue Analysis. Blood samples and liver tissue were collected under deep anesthesia after a 8-h fast. Serum alanine aminotransferase (ALT), aspartate aminotransferase (AST), glucose and cholesterol levels were measured using Roche-Hitachi 911 Chemistry Auto-Analyzer. Plasma insulin was measured using a mouse insulin enzymelinked immunosorbent assay kit (Milipore). Insulin resistance was calculated using the homeostasis model assessment of insulin resistance (HOMA-IR) [31]. Whole liver were homogenized in 1 mL of cold lysis buffer (50 mM HEPES [pH 7.5], 150 mM NaCl, 1 mM ethylenediaminetetraacetic acid (EDTA), 2.5 mM ethyleneglycol tetraacetic acid [EGTA], 1 mM dithiothreitol, 10% glycerol, 1 mM phenylmethylsulfonyl fluoride [PMSF], 10 μg/mL each of aprotinin and leupeptin, 50 mM NaF and 0.1 mM sodium orthovanadate) per 100 mg of tissue [32]. Homogenates were clarified by centrifugation at 10,000g for 10 minutes at 4°C and stored at -70°C. Thiobarbituric acid reactive substances (TBARS) assay were measured to quantify lipid peroxidation and tissue oxidative stress in whole liver homogenate using a colorimetric assay as described by Ohkawa et al [33]. Commercial ELISA kits were used to measure hepatic levels of TNF-alpha (Mouse TNF-α ELISA Kit, EZMTNFA, Milipore) and MCP-1 (Mouse MCP-1 Elisa kit, RAB0056, Sigma) following the manufacturers' instructions. Hepatic lipid content was analyzed for total triglycerides (TG) and cholesterol, briefly, frozen liver tissue (100 mg) was homogenized in 1.6 ml phosphate-buffered saline and protein concentration was determined using Bradford Protein Assay (Bio-Rad). Lipid was extracted using chloroform:methanol (2:1) and 0.1% sulfuric acid as described [34]. An aliquot of the organic phase was collected, dried with chloroform containing 1% Triton, and resuspended in water (final Triton concentration =

~2%). TG content was determined using commercially available kits (Wako Chemicals) in microtiter plates and normalized to protein concentration of the homogenate. The hepatic lipid concentration was expressed as μg of TG/mg of liver protein.

Terminal Deoxynucleotidyl Transferase–Mediated dUTP Nick-End Labeling (TUNEL) Assay. Tissue sections (5 μm) were prepared, and terminal deoxynucleotidyl transferase dUTP nick-end labeling (TUNEL) assay was performed following manufacturer's instructions (ApopTag Fluorescein In Situ Apoptosis Detection Kit, Chemicon). Apoptotic cells were quantified by the TUNEL assay, which enzymatically labels free 3'-OH ends of damaged DNA with a fluorescently labeled nucleotide as we have previously described in detail[35]. TUNEL-labeled cells (that is, fluorescent nuclei) were quantified by the number of positive cells per high-power field being counted. A total of 10 high-power fields were analyzed for each animal, using Nikon Eclipse E800 microscope (Nikon, Melville, NY) coupled to a Nikon DN100 CCD camera. Data were expressed as the number of TUNEL-positive cells per 10 high-power fields.

α-Smooth Muscle Actin Staining. Livers were dissected and processed for paraffin inclusion. Five micron-thick sections of formalin-fixed, paraffin-embedded liver were used for α-SMA immunofluorescence staining. Slides were deparaffinized in xylene and serially rehydrated in graded ethanol (100 to 70%). Endogenous peroxidase was quenched with 0.5% hydrogen peroxide in 90% ethanol for 20 min. Prior to primary antibody incubation,

endogenous avidin and biotin were blocked for 20 min using the Vector Laboratories blocking kit and unspecific binding of the antibody was subsequently blocked for 30 min in 1% BSA in PBS. Tissue was incubated overnight with a mouse monoclonal Cy3-coupled anti-smooth muscle actin antibody (αSMA; 1/200; Sigma). After extensive washing, sections were coverslip-mounted for microscopic observation. As technical control, incubation with primary antibody was omitted rendering no significant staining. Pictures were taken using a Nikon DN100 CCD camera coupled to a Nikon Eclipse 800 fluorescence microscope. Quantitative analysis of immunohistochemical staining of αSMA was performed by computerized morphometric analysis (CMA). Approximately 100-200 microscopic field (x400) per specimen were captured and analyzed using a color threshold detection system developed in Matlab 6.0 (Mathworks,Inc, USA). The results obtained were expressed as unit of αSMA positive area per field.

Assessment of Liver Fibrosis. Liver fibrosis was semiquantified using Sirius red staining as described by Camino et al [36]. Liver sections were stained with picrosirius red staining, and red-stained collagen fibers were quantified by computerized morphometric analysis (CMA). For CMA whole liver samples were analyzed with the excepetion of large centrilobular veins and large portal tract (≥ 150 μm). Two hundred light microscope images per speciem were captured and analyzed using color threshold detection system (Matlab 6.0, Mathworks,Inc, USA). The results were expressed as a percentage of positive area.

Additionally, collagen deposition was measured by hydroxyproline assay as detailed previously [36]. Briefly, hydroxyproline content was quantified colorimetrically in duplicate from 0,2 g liver sample at 557 mm from a standard curve the amino acid alone and against a blank reagent. The results were expressed as mg/g of liver tissue.

Histopathology. For histological review of hematoxylin and eosin (H&E)–stained liver sections by light microscopy (Eclipse, Nikon), the liver was fixed in 10% formalin buffer, and then embedded in paraffin. Tissue sections of 5-μm-thick were prepared and placed on glass slides. H&E and Mallory Trichrome staining were performed according to standard techniques. The slides were coded, without the pathologist knowing the specific treatment group that the slides represented. The histology was graded according to a number of histological features. Steatohepatitis was assessed using NAFLD activity score by the modified semiquantitative Brunt score [37]. This measures degree of steatosis (0= <5%; 1: 5%-33%; 2= 33%-66%; 3= >66%), inflammation (0= no foci; 1= <2 foci per 200x field; 2= 2-4 foci per 200x field; 3= >4 foci per 200x field), and hepatocyte ballooning degeneration (0= none; 1= few balloon cells; 2= many cells/prominent ballooning). Fibrosis was determined by the following scale, 0= none; 1= zone 3 only, perisinusoidal; 2= zone 2-3, perisinusoidal; 3= perisinusoidal and portal/periportal; 4= bridging fibrosis; 5= cirrhosis.

Analysis of Caspase Activation. For detection of the active form of caspases-3 and -8, colorimetric protease assay kits (Chemicon International, Inc.) were used. Proteins obtained from cytosolic extracts from liver tissue (100 μg) and were incubated with 200

μM DEVD-pNA (for caspase-3) or IETD-pNA (for caspase-8), The assay was based on the spectrophotometric detection of the chromophore p-nitroanilide (pNA) after cleavage from the labeled substrates. p-NA light emission was quantified using a microtiter plate reader at 405 nm. Comparison of the absorbance of p-NA from HFD fed mice samples with regular chow fed mice allowed determination of the-fold increase in caspase activity [38], samples were evaluated in triplicate each.

Real-Time Polymerase Chain Reaction. Total RNA was extracted from liver tissue using the Trizol Reagent (Invitrogen), and was reverse-transcribed into complementary DNA with Moloney leukemia virus reverse transcriptase and random primers (both from Invitrogen). Quantification of the complementary DNA template was performed with real-time polymerase chain reaction (PCR) (Mx3000P QPCR thermocycler, Stratagene) using SYBR green (Invitrogen) as a fluorophore. PCR primers (all obtained from Invitrogen) were as follows: murine αSMA Forward: 5′-ACT ACT GCC GAG CGT GAG AT-3′, Reverse: 5′-AAG GTA GAC AGC GAA GCC AG-3′; murine Collagen1-α Forward: 5′-GAA ACC CGA GGT ATG CTT GA-3′, Reverse: 5′-GAC CAG GAG GAC CAG GAA GT-3′; murine Interleukin-1β Forward: 5′- GCC CAT CCT CTG TGA CTC AT-3′, Reverse: 5′-AGG CCA CAG GTA TTT TGT CG-3′; murine CHOP Forward: 5′- CTG CCT TTC ACC TTG GAG AC-3′, Reverse: 5′-GGA CGC AGG GTC AAG AGT AG-3′; murine TGF-β Forward: 5′- CTC CCG TGG CTT CTA GTG C-3′, Reverse: 5′-GCC TTA GTT TGG ACA GGA TCT G-3′, murine TNF-α: Forward 5′- CCC TCA CAC TCA GAT CAT CTT CT-3′, Reverse: 5′-GCT ACG ACG TGG GCT ACA G-3′; murine TIMP-1: Forward 5′-CAT GGA AAG CCT CTG TGG ATA TG-3′, Reverse: 5′-GAT GTG CAA ATT TCC GTT CCT T-3′;

murine CXCL-2: Forward 5'-CTC TCA AGG GCG GTC AAA AAG TT-3', Reverse: 5'-TCA GAC AGC GAG GCA CAT CAG GTA-3'; murine MCP-1: Forward 5'- CTT CTG GGC CTG CTG TTC A-3', Reverse: 5'-CCA GCC TAC TCA TTG GGA TCA-3'. As an internal control, primers from murine β-Actin were used as follow: Forward: 5'- TTC TAC AAT GAG CTG CGT GT-3', Reverse: 5'-CTC TCA GCT GTG GTG GTG AA-3'. After electrophoresis in 1,5% agarose gel, each expected base pair PCR product was cut out and eluted into Tris-HCl using a DNA elution kit (Gel extraction kit; Quiagen). The concentrations of extracted PCR products (copies per microliter) were measured using a spectrophotometer at 260 nm and were used to generate standard curves. The inverse linear relationship between copy and cycle numbers was then determined. Each resulting standard curve was then used to calculate the number of copies per microliter in experimental samples. The relative expression level of each product was expressed as a ratio of β-Actin copies of PCR Product for each sample. Data were expressed as fold change from regular chow fed mice.

Statistical Analysis. All data represent are expressed as the mean ± 95% CI for mean, or otherwise indicated. Differences between groups were compared by an ANOVA analysis followed by a post-hoc Student-Newman–Keuls test, parametric test or the Kruskall–Wallis nonparametric test. Differences were considered to be statistically significant at $P<0.05$.

RESULTS

Is Liver injury attenuated in Emricasan treated HFD fed mice?

We first examined the effects of the pan-caspase inhibitor Emricasan on hepatocyte apoptosis in C57BL/6J mice fed a high fat diet. Hepatocyte apoptosis was assessed by TUNEL assay and caspase -3 and -8 activities were evaluated to determine the efficiency of the pharmacological caspase inhibition by emricasan (Figure 1). TUNEL positive cells were considerably increased by 5 fold in mice fed a HFD and were reduced under emricasan treatment (Figure 1 A, and B). In accordance with this observation caspase -3 and -8 were increased in HFD-fed mice by 1.5 and 1.3 fold respectively and were significantly decreased by emricasan treatment (Figure 1 C and D). To further evaluate the effects of the pan-caspase inhibitor in reducing liver injury, we next examined liver histology score, serum AST and ALT values in HFD fed mice treated with vehicle or emricasan. Histopathologic examination of liver specimens demonstrated increased histological parameters of liver injury as assessed by NAFLD activity score (NAS) in the mice fed a HFD (Figure 2). In accord with this observation, serum AST and ALT were 3-5 fold higher in HFD than regular chow-fed mice, and the emricasan treated group showed a significant decrease in AST and ALT serum levels (Figure 3 A and B). Also, Lipid peroxidation was assessed as a surrogate for hepatic oxidative stress-mediated liver injury. Significantly higher levels of TBARS were detected in HFD-fed animals compared to regular chow diet, and the emricasan treatment significantly reduced TBARS (Figure 3 C).

Next we evaluated the effect of emricasan on features of metabolic syndrome and hepatic steatosis. Mice fed a HFD had significantly increased weights, associated with

hyperglycemia, hyperinsulinemia and hypercholesterolemia as compared with regular chow-fed mice (Table 1). Moreover, HFD-fed mice had dramatically induced fat accumulation, increasing the score of steatosis (Figure 2) and hepatic content of triglycerides and cholesterol (Table 1). Treatment with emricasan did not significantly impact features of metabolic syndrome, insulin resistance or hepatic steatosis. Collectively, these data indicate a pathogenic role for caspase-mediated hepatocyte apoptosis in liver injury in a NASH murine model and demonstrate that the pan-caspase inhibitor emricasan decreases liver injury but not metabolic derangement in NASH.

Is hepatic inflammation reduced in Emricasan-treated HFD-fed mice?

To examine the changes of hepatic inflammation in HFD fed mice under Emricasan treatment, key mediators of inflammation (TNF-α, IL-1β), monocyte and neutrophil infiltration (MCP-1, CXCL2) were quantitated at protein level and messenger RNA transcripts using qPCR. In HFD fed mice, the inflammatory mediators TNF-α, IL-1β, MCP-1 and CXCL2 were significantly increased compared with Emricasan-treated HFD fed animals (Fig. 4, A, B, C, D, E and F). Consistent with these results, histological examination of inflammation score demonstrated a clear decrease in inflammatory foci in emricasan-treated mice compared with vehicle-treated HFD fed mice (Reg Chow: 0.3 ± 0.1, HFD: 2.2 ± 0.2*, HFD-Emricasan: 0.6 ± 0.2, * $p<0.05$) (Figure 2). Indeed the overall NAS score showed a protective effect by emricasan treatment (Reg Chow: 0.5 ± 01, HFD: 6.1 ± 0.3, HFD + Emricasan: 3.2 ± 0.4) (Figure 2). Such differences cannot be attributed to differences in hepatic steatosis as hepatic triglyceride content was similar in both groups

(Table 1). Therefore, these data demonstrate that inflammation is coupled to caspase-dependent liver injury in HFD-diet induced NASH and the treatment with the pan-caspase inhibitor ameliorates inflammation and liver injury.

Is hepatic fibrogenesis attenuated in Emricasan treated HFD fed mice?

To investigate if the reduction in liver injury in HFD-fed mice with Emricasan is significant, it should also translate into reduced hepatic fibrogenesis. Because phagocytosis of apoptotic bodies promotes myofibroblastic transformation of HSC, we next evaluated α-SMA expression, an established marker for HSC activation in NASH [39], by quantifying mRNA transcripts with qPCR analysis. In HFD-fed animals, α-SMA mRNA transcripts were significantly increased compared with regular chow group, indicating HSC activation in NASH (Figure 5 A). In contrast, the transcripts for α-SMA were significantly reduced by 80% in Emricasan-treated HFD-fed animals compared with vehicle-treated HFD mice (Figure 5 A). These results were confirmed at the cellular level by performing α-SMA immunohistochemistry. Consistent with the mRNA data, the number of α-SMA-positive cells was increased along hepatic sinusoid lining cells in HFD-fed mice, and was dramatically reduced in drug-treated HFD mice and was confirmed by morphometric analysis (Figure 5 B and C). To ascertain whether other markers for HSC activation were also reduced in emricasan-treated HFD mice, transcripts for molecules implicated in fibrogenesis were quantified. TGF-β and TIMP-1, pivotal cytokines in promoting fibrogenesis, were also increased in HFD animals versus Emricasan-treated HFD mice (Figure 6 A and B).

To determine if the reduced α-SMA expression was accompanied by changes in liver fibrosis, collagen-1α (I) mRNA expression, the principal form of collagen in hepatic cirrhosis, was determined using qPCR techonology. Indeed, collagen-1α was clearly increased by 5-fold in HFD-fed mice versus Emricasan-treated mice (Figure 7 B). Furthermore, liver specimens were analyzed by Mallory´s trichrome and collagen deposition was stained using Sirius red and quantitated by digital image analysis (Figure 7 A). Liver histology evaluation by Mallory´s trichrome observed evidence of perisinusoidal and pericellular fibrosis in HFD animals, as expected in NASH; in comparision, the amount of fibrosis was significantly reduced in HFD-fed mice treated with Emricasan (Modified fibrosis score: HFD: 2,3±0,3 Vs HFD-Emricasan: 0,3±0,2, $p<0,001$), and no fibrosis was observed in regular chow fed mice (Figure 7 A and C). Sirius red staining showed significant collagen staining like “chicken wire” along sinusoids (perisinusoidal) and around hepatocytes (pericentral) in HFD-fed mice; however, the quantity of collagen was again significantly reduced in Emricasan-treated mice (Figure. 7 A and D). Accordingly, the biochemical assessment of hydroxyproline showed a marked increase in the mean hydroxyproline levels by 8-fold in HFD-fed animals than in the Emricasan-treated mice (Figure 7 E). Collectively, these observations suggest that, in the murine NASH model, stellate cell activation and hepatic fibrogenesis are attenuated by administration of the pan-caspase inhibitor Emricasan.

DISCUSSION

The principal findings of this study pertain to the role of caspase inhibition as a therapeutic pharmacological target in a murine model of metabolic syndrome with NASH. We demonstrate that prolonged pharmacological inhibition of caspases has a beneficial effect in NASH by reducing hepatocyte apoptosis and decreasing liver injury, hepatic inflammation and markedly reducing HSC activation and fibrogenesis. Together these observations suggest caspase activation has a clear pathogenic role in NASH and a treatment that inhibits hepatocyte apoptosis might limit hepatic injury and attenuate progression of fibrosis in NASH, a highly prevalent disease with no effective pharmacological therapy.

In this study we used a high fat diet that recapitulates the clinical findings in human NASH such as obesity and insulin resistance [29 30]. This diet also was enriched in fructose and cholesterol, two key components of the western diet induced NASH [40 41] that are associated with liver injury [42 43], inflammation [44 45] and fibrosis [46 47]. Moreover, in our study the histopathological analysis of the liver specimens from HFD-fed mice depicts the characteristic features of NASH which are para-acinar steatosis, cellular ballooning, acinar inflammation, hepatocyte apoptosis, peri-sinusoidal and peri-celluar fibrosis [48 5]. Thus, our diet induced NASH is a useful tool to examining therapeutic approaches during metabolic disturbances.

Apoptosis has been implicated as cardinal feature of non-alcoholic fatty liver disease by serological markers and liver tissue analysis, where it correlates with histological severity and fibrosis progression [5 6]. Hepatocyte apoptosis in vitro and in murine models of

steatohepatitis is mediated in part by the activation of the extrinsic pathway of apoptosis by death receptor Fas [49 5] and TRAIL-DR4/TRAIL-DR5 [8 9 10], that can be activated by their ligands but also the toxic saturated fatty acid palmitate can activate TRAIL-DR5 by clustering [50] and augment the FADD-recruitment and caspase-8 activation of Fas by palmitoyltation [51]. In vitro studies demonstrate that free fatty acids induce hepatocyte apoptosis by activation of the intrinsic pathway; the saturated fatty acids trigger ER stress-associated JNK and CHOP activation engage apoptosis by enhancing expression and function of pro-apoptotic members of the Bcl-2 family, PUMA [12 52] and Bim [53 54]. Both apoptotic pathways converge on caspase activation to induce cell death, and based on this concept the use of pharmacological inhibition of caspase is a useful tool to reduce hepatocyte apoptosis. In this study we demonstrate a significant increase in hepatocyte apoptosis and caspase activation in the NASH model of HFD-fed mice, and the treatment with emricasan, a pan-caspase inhibitor, abrogates liver cell apoptosis and caspase activation evaluated by TUNEL assay and caspase-3 and -8 activities. Our observations support previous in-vitro studies that showed FFA mediated cytotoxicity was completely blocked by a pan-caspase inhibitor [11] and a NASH clinical trial where use of the caspase inhibitor GS-9450 decreased cytokeratin-18 fragments, a serum marker of hepatocytes apoptosis [55].

In liver, hepatocyte apoptosis has been linked to inflammation and fibrogenesis. The mechanisms by which apoptosis promotes inflammation relate to the engulfment of apoptotic bodies by monocyte/macrophage resident cells (Kupffer cells), engaging their activation and expression of death ligands (TNF-α, TRAIL and FasL) [19], pro-inflammatory

cytokines and chemokines [56]. These recruit and activate inflammatory cells that may further aggravate liver inflammation, what is called the second phase of injury. In contrast to a decreased liver injury, we failed to observe a reduction in hepatic steatosis. This is not unexpected, since triglyceride synthesis has been suggested as a protective mechanism against lipotoxicity [57]. Indeed, these observations is in accord with Anstee et al [25] that using a mice fed a high fat diet under the pan-caspase inhibitor VX-166 showed a marked decreased in hepatocyte apoptosis with no effect on liver steatosis, also in a NASH clinical trial [55] no effect was observed in parameters associated with metabolic syndrome using a pan-caspase inhibitor GS-9450. Our study is consistent with an anti-inflammatory effect of pan-caspase inhibitor treatment. In mice fed a HFD we observed a clear inflammatory milieu, with increased inflammatory foci in liver specimens, oxidative stress and elevated level of pro-inflammatory cytokines TNF-α and IL1-β, and chemokines CXCL2 and MCP-1. The pan-caspase inhibitor abrogates the induction of the pro-inflammatory cytokines and chemokines by HFD, and markedly reduced the inflammatory score of liver sections. Possibly, this phenomenon could be associated with inhibition of pro-inflammatory caspases, like caspase-1, -4, -5 and -11. In this way, recent data support a pro-inflammatory effect of caspase-1 in diet induced NASH [58]; in this work murine *casp-1 -/-* showed a decreased expression of pro-inflammatory cytokines, however there was no effect on hepatocyte apoptosis or serum aminotransferase levels. The current study extends this observation by demonstrating a reduction of aminotransferase and hepatocyte apoptosis under pan-caspase therapy in diet induced NASH. Also, our results support the data of Csak et al [59], that used an in-vitro model of free fatty acids induced

cytotoxicity, where a pan-caspase inhibitor decreased IL1-β production and inflammasome activation of steatotic hepatocytes. Perhaps, blocking pro-apoptotic caspases would have a hepatocyte-cytoprotective effect and inhibition of pro-inflammatory caspases might prevent the second phase of injury. Future investigation will be necessary to elucidate the biological and clinical importance of each caspase in the pathogenesis and therapy of NASH.

Recently the importance of adipokines in the development of hepatic steatosis and steatohepatitis has been recognized [60]. Adipokines are polypeptides secreted in the adipose tissue in a regulated manner. Changes in levels of leptin, adiponectin, visfatin, resistin and TNF have been linked to the development of insulin resistance, obesity, and liver steatosis; an imbalance in these factors could potentially contribute to the initiation and progression of fatty liver disease [61]. It is beyond the scope of this work to address the impact of caspase inhibition on adipokines levels. However recent data from Dixon et al have shown that total body adipose volumes were increased in Casp1-/- mice on the high fat diet to a greater extent than wild-type mice. Indeed subcutaneous adipose, rather than visceral adipose tissue, is increased in Casp1-/- mice on high fat diet [62]. Perhaps, these shifts in adipose accretion to subcutaneous adipose tissue could modulate adipokines levels and may protect from diet-induced steatohepatitis in caspase1-deficient mice.

As previously reported [22 24], this study demonstrates that pan-caspase inhibitor treatment improved hepatic fibrogenesis. Witek et al, using the obese leptin receptor deficient *db/db* mice fed methionine/choline-deficient diet (MCD) for 8 weeks under pan-caspase inhibitor

VX-166 showed a marked decrease in HSC activation and fibrosis. Canbay et al [22], reported in a murine model of cholestasis, using bile duct ligation (BDL), a marked reduction in HSC activation and collagen-1α deposition. Our study, using a HFD induced NASH with prolonged emricasan treatment, demonstrated a significant inhibition of HSC activation, reduced pro-fibrogenic cytokine expression, and marked improvement in fibrosis by reduced collagen-1α deposition and hydroxyproline liver content. The mechanism involved in this anti-fibrotic effect perhaps is related to the anti-inflammatory and anti-hepatocyte apoptotic effect offered by pan-caspase inhibition. In this way, by reducing apoptotic bodies and decreasing the secondary inflammatory response, HSC activation is abolished and liver fibrosis prevented. The limits of the present study pertain to the experimental model used; we administered emricasan in conjunction with the HFD, leaving the question if the previously deposited collagen could be improved or not in well established fibrosis. One possibility is that emricasan, by limiting further injury, prevents inflammatory cell recruitment/activation, decreases the expression of TIMP-1, promotes HSC apoptosis and enhances matrix resorption [63 64 65]. Additional studies using models of chronic fibrosis and cirrhosis will be necessary to evaluate the effects of Emricasan in established fibrotic models.

Although long-term use of antiapoptotic agents raises the theoretical concern of increased risk of neoplastic transformation, this is unlikely. Whereas physiologic apoptosis helps protect from cancer, excessive apoptosis might, at least in some experimental situations, enhance neoplastic transformation [66]. This was depicted by Weber et al, in mice lacking the a anti-apoptotic factor myeloid cell leukemia-1 (Mcl-1), have increased apoptosis, cell

turnover, which translates into development of malignant HCC-like lesions [67]. Also, in the transgenic mice that over expressed Bcl-2 in the liver, HCC was prevented in transforming growth factor-alpha-induced genetic mouse model of HCC [68]. Consistent with this data, deletion of proapoptotic BH-3-only protein PUMA protect against diethyl nitrosamine (DEN) induced liver cancer [69]. Moreover, loss of the death receptor Fas also inhibits DEN induced carcinogenesis [70]. Along these lines, knockout murine models of various death receptors do not develop spontaneous cancers. Based on this concept, persistent hepatocyte apoptosis promotes inflammation and associated compensatory cellular proliferation, increasing the risk of hepatic carcinogenesis. Thus abrogating apoptosis in chronic liver inflammation by caspase inhibitors should be safe with regard to cancer risk. Extrapolation of these interesting findings to human disease states should be carefully addressed in future investigations of this class of drugs.

In summary, our results suggest the following scenario of liver protection by Emricasan in NASH: in the murine model of HFD diet induced NASH, cell damage or cell death products results in the production by inflammatory cells of pro-inflammatory cytokines and chemokines, triggering a pro-inflammatory milieu that further increases hepatocyte damage and inflammation. This phenomenon activates HSC by phagocytosis of apoptotic bodies and releasing of the pro-fibrogenic cytokines by inflammatory cells, thus accelerating production of extracellular matrix by collagen-1α, TIMPs and cytokines and promoting liver fibrosis of the liver. The pan-caspase inhibitor emricasan was found to suppress hepatocyte apoptosis by blocking pro-apoptotic caspases; this decrease in cell

damage and the inhibition of pro-inflamatory caspases may then interrupt the inflammatory milieu and prevent a pro-fibrogenic process and activation of HSC. Therefore, the use of a pan-caspase inhibitor might provide an attractive anti-fibrotic therapy in NASH.

TABLES.

Table 1. Metabolic biochemical profile

	Reg Chow	HFD	HFD + Emricasan
Final weigth (g)	**31 ± 1**	**43 ± 2 ****	**42 ± 2 ****
Glucose (mg/dl)	**208 ± 16**	**302 ± 30 ***	**281 ± 23 ***
Insulin (mU/mL)	**17 ± 3**	**37 ± 4 ****	**35 ± 5****
HOMA-IR	**8 ± 3**	**28 ± 10****	**24 ± 8****
Serum Cholesterol (mg/dl)	**68 ± 10**	**183 ± 25 ****	**141 ± 7 ****
Liver triglycerides	**50 ± 5**	**89 ± 11 ***	**96 ± 11 ***

(mg/g)			
Liver cholesterol (mg/g)	**5 ± 2**	**12 ± 2 ****	**9± 2 ****

Values are means ± SD, * p < 0.05, ** p < 0.001

DISCLOSURES: We have no conflict of interest associated with this publication

FUNDING: This work was supported by a grant from Agencia Nacional para la Promocion Cientifica y Tecnologica (Foncyt, PICT-O UNAM-2011). The funder had no role in study design, data collection and analysis, decision to publish, or preparation of the manuscript.

ACKNOWLEDGMENTS: Dr Barreyro wants to thanks Prof Raul Marucci, Prof Juan Sorda and Dr Esteban Gonzalez Ballerga for their strong support

FIGURE LEGENDS

FIGURE 1. **Hepatocyte apoptosis and caspase activation are attenuated in Emricasan treated HFD-fed mice.** *A*: Representative photpmicrograoh of TUNEL-stained liver sections are shown. *B*: The number of TUNEL-positive cells (marked with arrows) was quantitated

and expressed as apoptotic cells/high-power fields (HPF). *C*: Apoptosis was also evaluated by measuring caspase-3 biochemical activity (Percentage of activity from Reg Chow mice) and *D:* by measuring caspase-8 biochemical activity (Percentage of activity from Reg Chow mice). Data are expressed as the mean +/- 95% CI for mean. *p< 0.05. Regular Chow-fed mice (C), High Fat Diet-fed mice (HFD) and emricasan treated High Fat Diet-fed mice (HFD + Emricasan).

FIGURE 2. **Pan-caspase inhibitor decrease the histopathological NAS score.** *A*: Representative hematoxylin-eosin stained sections of the liver at 100X and 400X. Liver sections were evaluated using the NAS (Non-alcoholic fatty liver disease Activity Score) histological score. Data represent mean ± standard error of the mean. * p<0.05. Regular Chow-fed mice (C), High Fat Diet-fed mice (HFD) and Emricasan treated High Fat Diet-fed mice (HFD + Emricasan).

FIGURE 3. **Serum markers of liver injury and hepatic oxidative stress are reduced in Emricasan treated HFD-fed mice** *A:* Serum AST and *B:* ALT values were measured. *C*: Hepatic TBARS levels were evaluated, fold change was determined after normalization to regular chow fed mice. Data are expressed as the mean +/- 95% CI for mean. * p< 0.05. Regular Chow-fed mice (C), High Fat Diet-fed mice (HFD) and Emricasan treated High Fat Diet-fed mice (HFD + Emricasan).

FIGURE 4. **Hepatic inflammatory mediators are reduced in Emricasan treated HFD-fed mice** *A:* TNF-alpha mRNA and *B:* TNF-alpha protein level values were measured by qPCR and ELISA. *C*: MCP-1 mRNA and *D:* MCP-1 protein level were measured by qPCR and ELISA. *E:* CXCL2 mRNA and *F:* IL-1β mRNA were quantified by qPCR. Data are expressed as the mean +/- 95% CI for mean. *p< 0.05. Regular Chow-fed mice (C), High Fat Diet-fed mice (HFD) and Emricasan treated High Fat Diet-fed mice (HFD + Emricasan).

FIGURE 5. **HSC Activation is attenuated in Emricasan treated HFD-fed mice.** *A*: mRNA was extracted from livers, αSMA mRNA expression, a marker of HSC activation, was quantified by qPCR. Fold induction was determined after normalization to Actin. *B:* Representative photomicrographs after immunofluorescence for αSMA are depicted (magnification 400X). C: morphometric analysis of quantitation αSMA + area is shown. C: Data are mean ± standard deviation. Asterisks indicate p<0.05. Regular Chow-fed mice (C), High Fat Diet-fed mice (HFD) and Emricasan treated High Fat Diet-fed mice (HFD + Emricasan).

FIGURE 6. **Pro-fibrogenic cytokine expression is reduced in Emricasan treated HFD-fed mice.** *A*: mRNA was extracted from livers and qPCR analyses of hepatic pro-fibrogenic cytokines were performed. Fold induction was determined after normalization to Actin. *A*: TGF-β, *B*: TIMP-1. Data represent mean ± standard deviation. * p<0.05. Regular Chow-fed mice (C), High Fat Diet-fed mice (HFD) and Emricasan treated High Fat Diet-fed mice (HFD + Emricasan).

FIGURE 7. **Liver fibrogenesis is attenuated under pan-caspase inhibitor treatment in HFD-fed mice.** *A*: Representative photomicrographs of Mallory's trichrome-stained (top) liver sections and Sirius red staining (bottom) a chemical stain of collagen deposition in the liver are shown. (magnification 400X) *B:* Collagen 1 (Coll-1) mRNA expression, marker of hepatic fibrogenesis, was quantified using qPCR, Fold induction was determined after normalization to Actin. *C:* Fibrosis was quantified using modified NAS histological score. *D:* Collagen fibers stained with Sirius red were quantified using digital image analysis in sinusoidal area. Representative photomicrographs of liver sections (left) are depicted (magnification 40X). (E) Hepatic hydroxyproline content. Data represent the mean ± standard deviation. * $p < 0.05$.

Figure 1

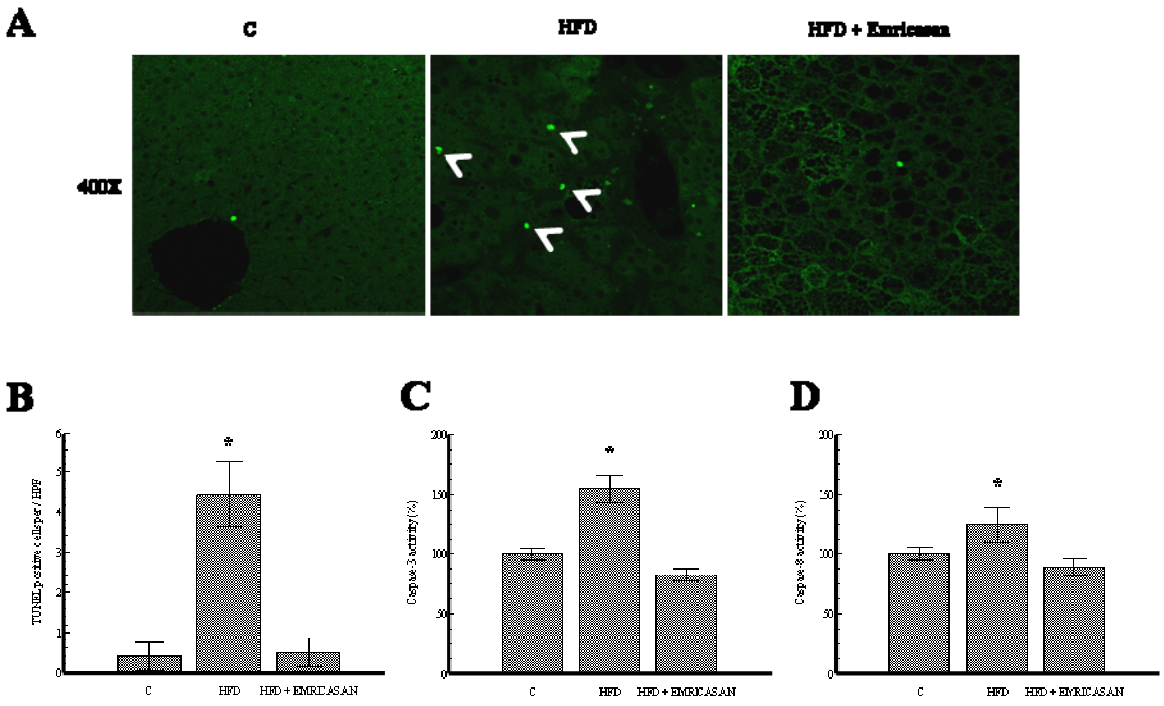

Figure 2

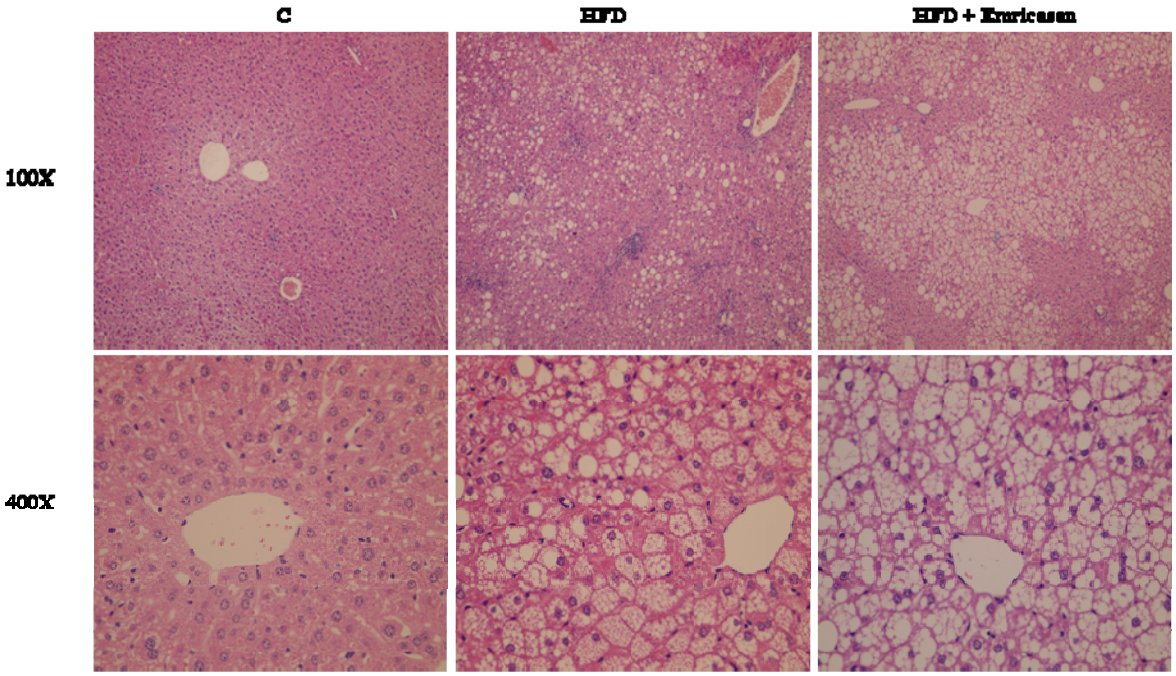

Score/Group	C	HFD	HFD + Emricasan
Steatosis	0.2 ± 0.1	2.7 = 0.1*	2.4 ± 0.1*
Inflammation	0.3 ± 0.1	2.2 = 0.2*	0.6 ± 0.2
Ballooning	0	1.2 = 0.2*	0.2 ± 0.1
NAS	0.5 ± 01	6.1 = 0.3*	3.2 ± 0.4*

Figure 3

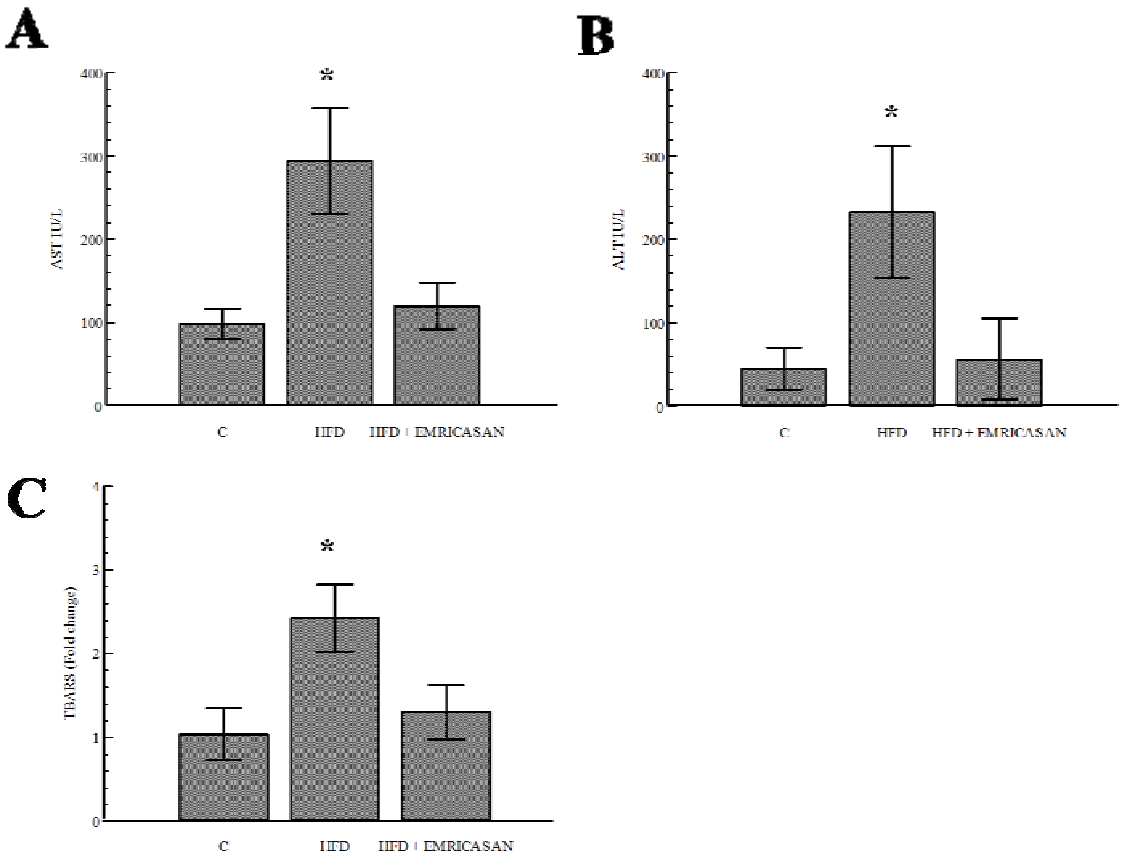

Figure 4

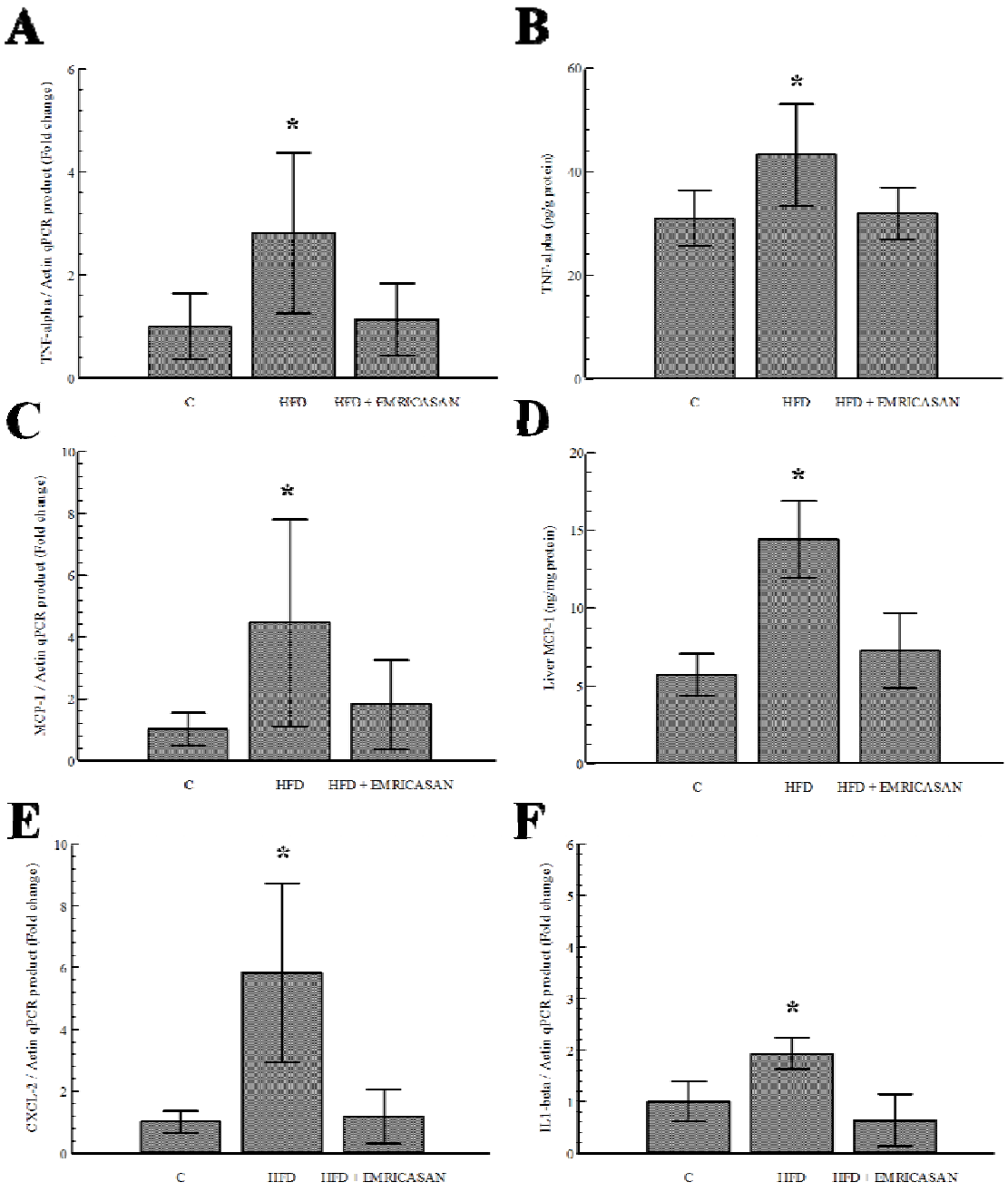

Figure 5

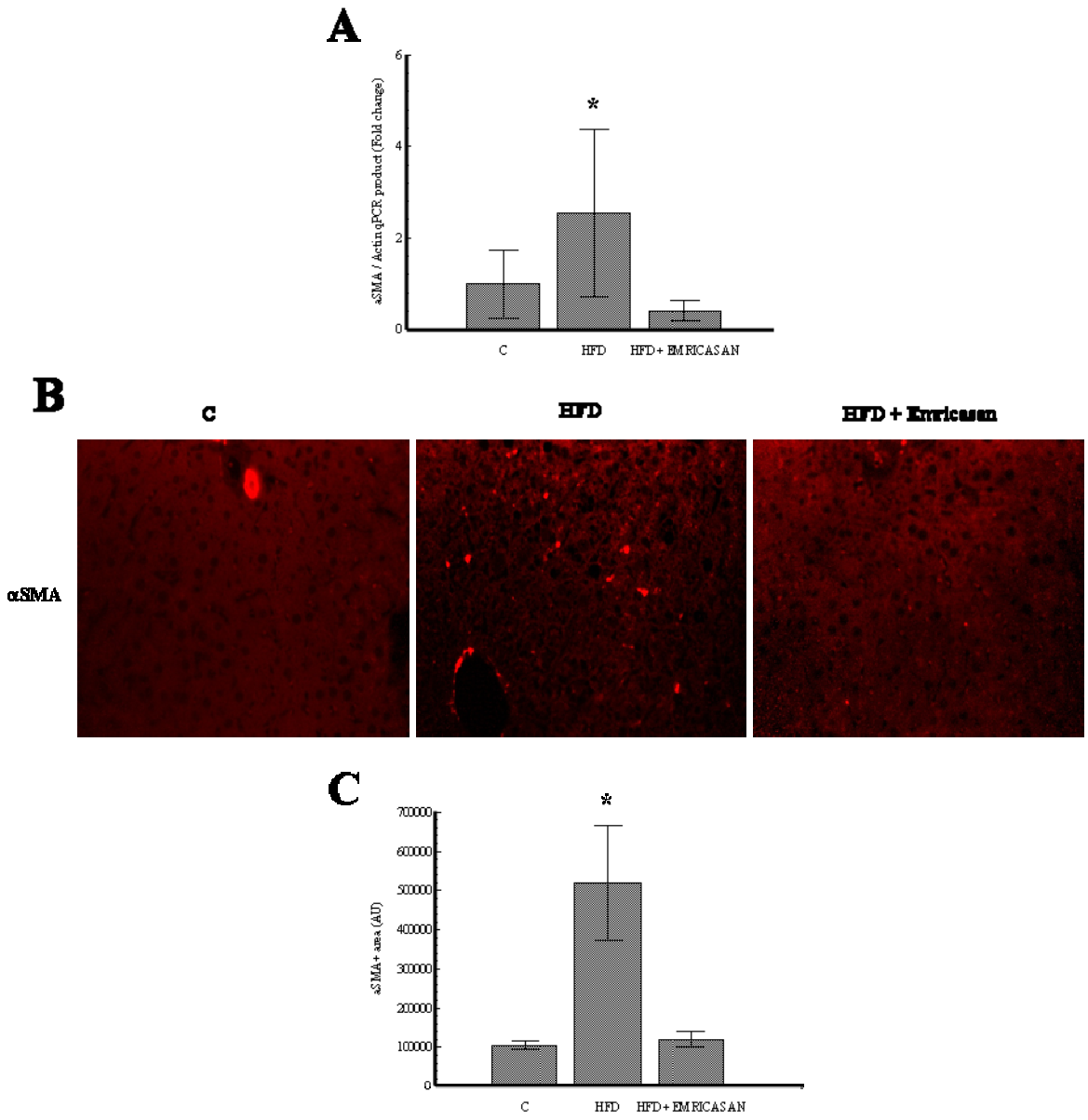

Figure 6

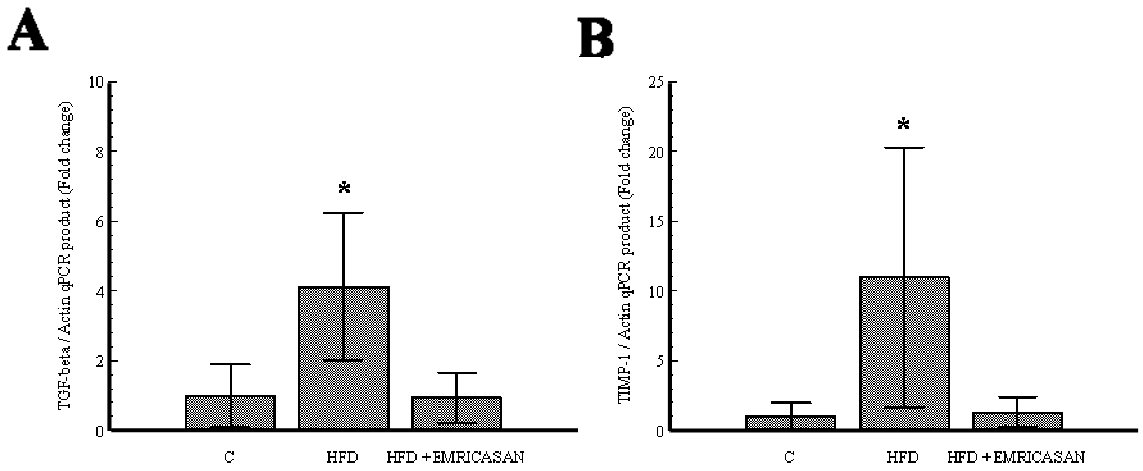

Figure 7

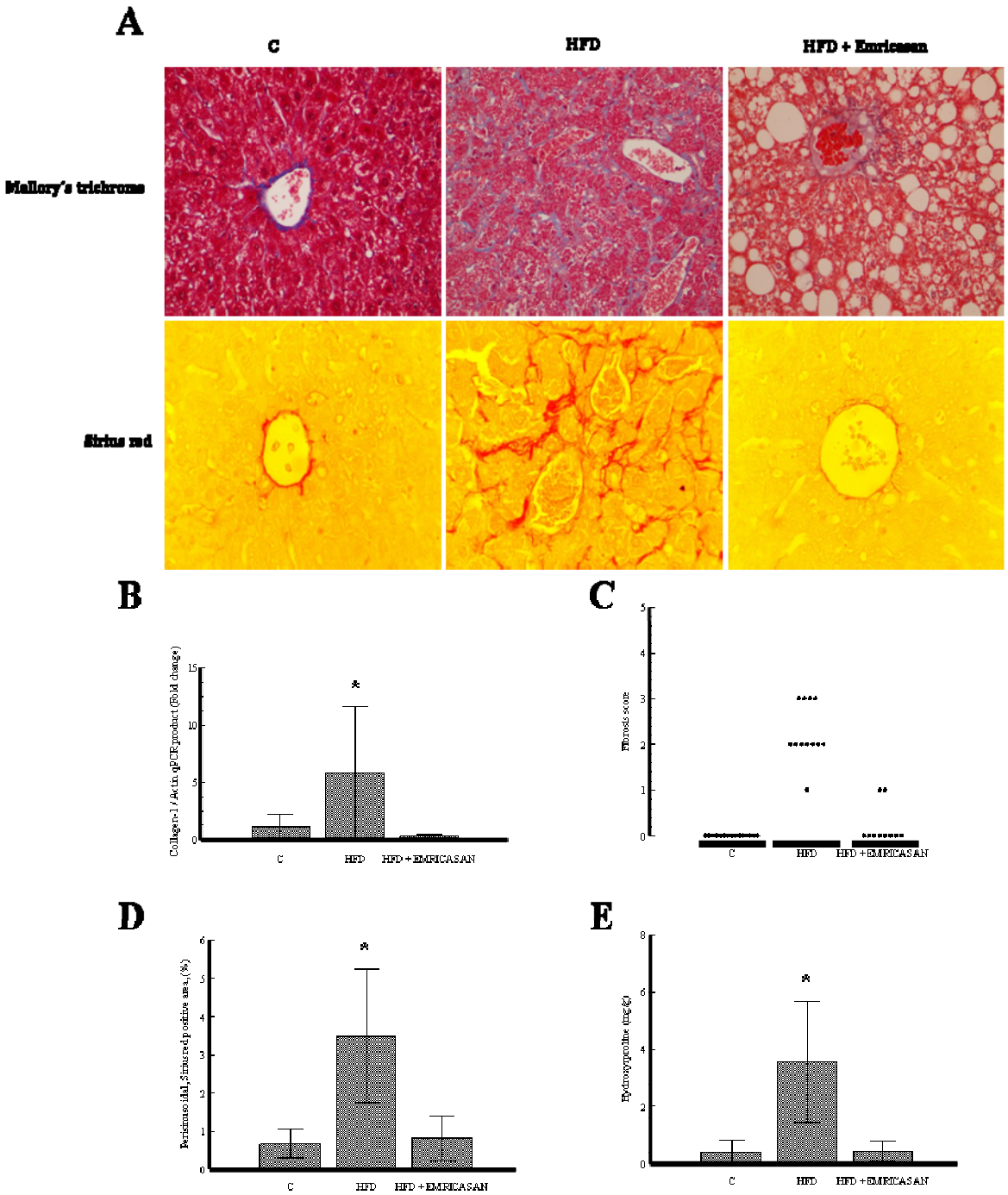

REFERENCES

1. Ratziu V, Bellentani S, Cortez-Pinto H, Day C, Marchesini G. A position statement on NAFLD/NASH based on the EASL 2009 special conference. J Hepatol;53:372-84.
2. Angulo P. Nonalcoholic fatty liver disease. N Engl J Med 2002;346:1221-31.
3. Chalasani N, Younossi Z, Lavine JE, Diehl AM, Brunt EM, Cusi K, Charlton M, Sanyal AJ. The Diagnosis and Management of Non-alcoholic Fatty Liver Disease: Practice Guideline by the American Gastroenterological Association, American Association for the Study of Liver Diseases, and American College of Gastroenterology. Gastroenterology;142:1592-609.
4. Vernon G, Baranova A, Younossi ZM. Systematic review: the epidemiology and natural history of non-alcoholic fatty liver disease and non-alcoholic steatohepatitis in adults. Aliment Pharmacol Ther;34:274-85.
5. Feldstein AE, Canbay A, Angulo P, Taniai M, Burgart LJ, Lindor KD, Gores GJ. Hepatocyte apoptosis and fas expression are prominent features of human nonalcoholic steatohepatitis. Gastroenterology 2003;125:437-43.
6. Wieckowska A, Zein NN, Yerian LM, Lopez AR, McCullough AJ, Feldstein AE. In vivo assessment of liver cell apoptosis as a novel biomarker of disease severity in nonalcoholic fatty liver disease. Hepatology 2006;44:27-33.
7. Feldstein AE, Canbay A, Guicciardi ME, Higuchi H, Bronk SF, Gores GJ. Diet associated hepatic steatosis sensitizes to Fas mediated liver injury in mice. J Hepatol 2003;39:978-83.
8. Malhi H, Barreyro FJ, Isomoto H, Bronk SF, Gores GJ. Free fatty acids sensitise hepatocytes to TRAIL mediated cytotoxicity. Gut 2007;56:1124-31.
9. Volkmann X, Fischer U, Bahr MJ, Ott M, Lehner F, Macfarlane M, Cohen GM, Manns MP, Schulze-Osthoff K, Bantel H. Increased hepatotoxicity of tumor necrosis factor-related apoptosis-inducing ligand in diseased human liver. Hepatology 2007;46:1498-508.
10. Farrell GC, Larter CZ, Hou JY, Zhang RH, Yeh MM, Williams J, dela Pena A, Francisco R, Osvath SR, Brooling J, Teoh N, Sedger LM. Apoptosis in experimental NASH is associated with p53 activation and TRAIL receptor expression. J Gastroenterol Hepatol 2009;24:443-52.
11. Malhi H, Bronk SF, Werneburg NW, Gores GJ. Free fatty acids induce JNK-dependent hepatocyte lipoapoptosis. J Biol Chem 2006;281:12093-101.
12. Cazanave SC, Mott JL, Elmi NA, Bronk SF, Werneburg NW, Akazawa Y, Kahraman A, Garrison SP, Zambetti GP, Charlton MR, Gores GJ. JNK1-dependent PUMA expression contributes to hepatocyte lipoapoptosis. J Biol Chem 2009;284:26591-602.
13. Feldstein AE, Werneburg NW, Canbay A, Guicciardi ME, Bronk SF, Rydzewski R, Burgart LJ, Gores GJ. Free fatty acids promote hepatic lipotoxicity by stimulating TNF-alpha expression via a lysosomal pathway. Hepatology 2004;40:185-94.
14. Wang D, Wei Y, Pagliassotti MJ. Saturated fatty acids promote endoplasmic reticulum stress and liver injury in rats with hepatic steatosis. Endocrinology 2006;147:943-51.
15. Li J, Yuan J. Caspases in apoptosis and beyond. Oncogene 2008;27:6194-206.

16. Martinon F, Tschopp J. Inflammatory caspases: linking an intracellular innate immune system to autoinflammatory diseases. Cell 2004;117:561-74.
17. Guicciardi ME, Gores GJ. Apoptosis: a mechanism of acute and chronic liver injury. Gut 2005;54:1024-33.
18. Martinou JC, Green DR. Breaking the mitochondrial barrier. Nat Rev Mol Cell Biol 2001;2:63-7.
19. Canbay A, Feldstein AE, Higuchi H, Werneburg N, Grambihler A, Bronk SF, Gores GJ. Kupffer cell engulfment of apoptotic bodies stimulates death ligand and cytokine expression. Hepatology 2003;38:1188-98.
20. Canbay A, Taimr P, Torok N, Higuchi H, Friedman S, Gores GJ. Apoptotic body engulfment by a human stellate cell line is profibrogenic. Lab Invest 2003;83:655-63.
21. Ueno Y, Ohmi T, Yamamoto M, Kato N, Moriguchi Y, Kojima M, Shimozono R, Suzuki S, Matsuura T, Eda H. Orally-administered caspase inhibitor PF-03491390 is retained in the liver for prolonged periods with low systemic exposure, exerting a hepatoprotective effect against alpha-fas-induced liver injury in a mouse model. J Pharmacol Sci 2007;105:201-5.
22. Canbay A, Feldstein A, Baskin-Bey E, Bronk SF, Gores GJ. The caspase inhibitor IDN-6556 attenuates hepatic injury and fibrosis in the bile duct ligated mouse. J Pharmacol Exp Ther 2004;308:1191-6.
23. Deaciuc IV, D'Souza NB, de Villiers WJ, Burikhanov R, Sarphie TG, Hill DB, McClain CJ. Inhibition of caspases in vivo protects the rat liver against alcohol-induced sensitization to bacterial lipopolysaccharide. Alcohol Clin Exp Res 2001;25:935-43.
24. Witek RP, Stone WC, Karaca FG, Syn WK, Pereira TA, Agboola KM, Omenetti A, Jung Y, Teaberry V, Choi SS, Guy CD, Pollard J, Charlton P, Diehl AM. Pan-caspase inhibitor VX-166 reduces fibrosis in an animal model of nonalcoholic steatohepatitis. Hepatology 2009;50:1421-30.
25. Anstee QM, Concas D, Kudo H, Levene A, Pollard J, Charlton P, Thomas HC, Thursz MR, Goldin RD. Impact of pan-caspase inhibition in animal models of established steatosis and non-alcoholic steatohepatitis. J Hepatol;53:542-50.
26. Linton SD, Aja T, Armstrong RA, Bai X, Chen LS, Chen N, Ching B, Contreras P, Diaz JL, Fisher CD, Fritz LC, Gladstone P, Groessl T, Gu X, Herrmann J, Hirakawa BP, Hoglen NC, Jahangiri KG, Kalish VJ, Karanewsky DS, Kodandapani L, Krebs J, McQuiston J, Meduna SP, Nalley K, Robinson ED, Sayers RO, Sebring K, Spada AP, Ternansky RJ, Tomaselli KJ, Ullman BR, Valentino KL, Weeks S, Winn D, Wu JC, Yeo P, Zhang CZ. First-in-class pan caspase inhibitor developed for the treatment of liver disease. J Med Chem 2005;48:6779-82.
27. Pockros PJ, Schiff ER, Shiffman ML, McHutchison JG, Gish RG, Afdhal NH, Makhviladze M, Huyghe M, Hecht D, Oltersdorf T, Shapiro DA. Oral IDN-6556, an antiapoptotic caspase inhibitor, may lower aminotransferase activity in patients with chronic hepatitis C. Hepatology 2007;46:324-9.
28. Shiffman ML, Pockros P, McHutchison JG, Schiff ER, Morris M, Burgess G. Clinical trial: the efficacy and safety of oral PF-03491390, a pancaspase inhibitor - a randomized placebo-controlled study in patients with chronic hepatitis C. Aliment Pharmacol Ther;31:969-78.

29. Vilar L, Oliveira CP, Faintuch J, Mello ES, Nogueira MA, Santos TE, Alves VA, Carrilho FJ. High-fat diet: a trigger of non-alcoholic steatohepatitis? Preliminary findings in obese subjects. Nutrition 2008;24:1097-102.
30. Solga S, Alkhuraishe AR, Clark JM, Torbenson M, Greenwald A, Diehl AM, Magnuson T. Dietary composition and nonalcoholic fatty liver disease. Dig Dis Sci 2004;49:1578-83.
31. Matthews DR, Hosker JP, Rudenski AS, Naylor BA, Treacher DF, Turner RC. Homeostasis model assessment: insulin resistance and beta-cell function from fasting plasma glucose and insulin concentrations in man. Diabetologia 1985;28:412-9.
32. Carreras MC, Converso DP, Lorenti AS, Barbich M, Levisman DM, Jaitovich A, Antico Arciuch VG, Galli S, Poderoso JJ. Mitochondrial nitric oxide synthase drives redox signals for proliferation and quiescence in rat liver development. Hepatology 2004;40:157-66.
33. Ohkawa H, Ohishi N, Yagi K. Assay for lipid peroxides in animal tissues by thiobarbituric acid reaction. Anal Biochem 1979;95:351-8.
34. Newberry EP, Kennedy SM, Xie Y, Sternard BT, Luo J, Davidson NO. Diet-induced obesity and hepatic steatosis in L-Fabp / mice is abrogated with SF, but not PUFA, feeding and attenuated after cholesterol supplementation. Am J Physiol Gastrointest Liver Physiol 2008;294:G307-14.
35. Kahraman A, Barreyro FJ, Bronk SF, Werneburg NW, Mott JL, Akazawa Y, Masuoka HC, Howe CL, Gores GJ. TRAIL mediates liver injury by the innate immune system in the bile duct-ligated mouse. Hepatology 2008;47:1317-30.
36. Camino AM, Atorrasagasti C, Maccio D, Prada F, Salvatierra E, Rizzo M, Alaniz L, Aquino JB, Podhajcer OL, Silva M, Mazzolini G. Adenovirus-mediated inhibition of SPARC attenuates liver fibrosis in rats. J Gene Med 2008;10:993-1004.
37. Kleiner DE, Brunt EM, Van Natta M, Behling C, Contos MJ, Cummings OW, Ferrell LD, Liu YC, Torbenson MS, Unalp-Arida A, Yeh M, McCullough AJ, Sanyal AJ. Design and validation of a histological scoring system for nonalcoholic fatty liver disease. Hepatology 2005;41:1313-21.
38. Matarrese P, Tinari A, Mormone E, Bianco GA, Toscano MA, Ascione B, Rabinovich GA, Malorni W. Galectin-1 sensitizes resting human T lymphocytes to Fas (CD95)-mediated cell death via mitochondrial hyperpolarization, budding, and fission. J Biol Chem 2005;280:6969-85.
39. Feldstein AE, Papouchado BG, Angulo P, Sanderson S, Adams L, Gores GJ. Hepatic stellate cells and fibrosis progression in patients with nonalcoholic fatty liver disease. Clin Gastroenterol Hepatol 2005;3:384-9.
40. Abdelmalek MF, Suzuki A, Guy C, Unalp-Arida A, Colvin R, Johnson RJ, Diehl AM. Increased fructose consumption is associated with fibrosis severity in patients with nonalcoholic fatty liver disease. Hepatology;51:1961-71.
41. Yasutake K, Nakamuta M, Shima Y, Ohyama A, Masuda K, Haruta N, Fujino T, Aoyagi Y, Fukuizumi K, Yoshimoto T, Takemoto R, Miyahara T, Harada N, Hayata F, Nakashima M, Enjoji M. Nutritional investigation of non-obese patients with non-alcoholic fatty liver disease: the significance of dietary cholesterol. Scand J Gastroenterol 2009;44:471-7.

42. Mari M, Caballero F, Colell A, Morales A, Caballeria J, Fernandez A, Enrich C, Fernandez-Checa JC, Garcia-Ruiz C. Mitochondrial free cholesterol loading sensitizes to TNF- and Fas-mediated steatohepatitis. Cell Metab 2006;4:185-98.
43. Pickens MK, Yan JS, Ng RK, Ogata H, Grenert JP, Beysen C, Turner SM, Maher JJ. Dietary sucrose is essential to the development of liver injury in the methionine-choline-deficient model of steatohepatitis. J Lipid Res 2009;50:2072-82.
44. Tetri LH, Basaranoglu M, Brunt EM, Yerian LM, Neuschwander-Tetri BA. Severe NAFLD with hepatic necroinflammatory changes in mice fed trans fats and a high-fructose corn syrup equivalent. Am J Physiol Gastrointest Liver Physiol 2008;295:G987-95.
45. Wouters K, van Gorp PJ, Bieghs V, Gijbels MJ, Duimel H, Lutjohann D, Kerksiek A, van Kruchten R, Maeda N, Staels B, van Bilsen M, Shiri-Sverdlov R, Hofker MH. Dietary cholesterol, rather than liver steatosis, leads to hepatic inflammation in hyperlipidemic mouse models of nonalcoholic steatohepatitis. Hepatology 2008;48:474-86.
46. Kohli R, Kirby M, Xanthakos SA, Softic S, Feldstein AE, Saxena V, Tang PH, Miles L, Miles MV, Balistreri WF, Woods SC, Seeley RJ. High-fructose, medium chain trans fat diet induces liver fibrosis and elevates plasma coenzyme Q9 in a novel murine model of obesity and nonalcoholic steatohepatitis. Hepatology;52:934-44.
47. Matsuzawa N, Takamura T, Kurita S, Misu H, Ota T, Ando H, Yokoyama M, Honda M, Zen Y, Nakanuma Y, Miyamoto K, Kaneko S. Lipid-induced oxidative stress causes steatohepatitis in mice fed an atherogenic diet. Hepatology 2007;46:1392-403.
48. Brunt EM, Neuschwander-Tetri BA, Oliver D, Wehmeier KR, Bacon BR. Nonalcoholic steatohepatitis: histologic features and clinical correlations with 30 blinded biopsy specimens. Hum Pathol 2004;35:1070-82.
49. Siebler J, Schuchmann M, Strand S, Lehr HA, Neurath MF, Galle PR. Enhanced sensitivity to CD95-induced apoptosis in ob/ob mice. Dig Dis Sci 2007;52:2396-402.
50. Cazanave SC, Mott JL, Bronk SF, Werneburg NW, Fingas CD, Meng XW, Finnberg N, El-Deiry WS, Kaufmann SH, Gores GJ. Death receptor 5 signaling promotes hepatocyte lipoapoptosis. J Biol Chem;286:39336-48.
51. Feig C, Tchikov V, Schutze S, Peter ME. Palmitoylation of CD95 facilitates formation of SDS-stable receptor aggregates that initiate apoptosis signaling. Embo J 2007;26:221-31.
52. Cazanave SC, Elmi NA, Akazawa Y, Bronk SF, Mott JL, Gores GJ. CHOP and AP-1 cooperatively mediate PUMA expression during lipoapoptosis. Am J Physiol Gastrointest Liver Physiol;299:G236-43.
53. Puthalakath H, O'Reilly LA, Gunn P, Lee L, Kelly PN, Huntington ND, Hughes PD, Michalak EM, McKimm-Breschkin J, Motoyama N, Gotoh T, Akira S, Bouillet P, Strasser A. ER stress triggers apoptosis by activating BH3-only protein Bim. Cell 2007;129:1337-49.
54. Barreyro FJ, Kobayashi S, Bronk SF, Werneburg NW, Malhi H, Gores GJ. Transcriptional regulation of Bim by FoxO3A mediates hepatocyte lipoapoptosis. J Biol Chem 2007;282:27141-54.
55. Ratziu V, Sheikh MY, Sanyal AJ, Lim JK, Conjeevaram H, Chalasani N, Abdelmalek M, Bakken A, Renou C, Palmer M, Levine RA, Bhandari BR, Cornpropst M, Liang W, King B, Mondou E, Rousseau FS, McHutchison J, Chojkier M. A phase 2, randomized, double-blind,

placebo-controlled study of GS-9450 in subjects with nonalcoholic steatohepatitis. Hepatology;55:419-28.
56. Geske FJ, Monks J, Lehman L, Fadok VA. The role of the macrophage in apoptosis: hunter, gatherer, and regulator. Int J Hematol 2002;76:16-26.
57. Choi SS, Diehl AM. Hepatic triglyceride synthesis and nonalcoholic fatty liver disease. Curr Opin Lipidol 2008;19:295-300.
58. Dixon LJ, Berk M, Thapaliya S, Papouchado BG, Feldstein AE. Caspase-1-mediated regulation of fibrogenesis in diet-induced steatohepatitis. Lab Invest;92:713-23.
59. Csak T, Ganz M, Pespisa J, Kodys K, Dolganiuc A, Szabo G. Fatty acid and endotoxin activate inflammasomes in mouse hepatocytes that release danger signals to stimulate immune cells. Hepatology;54:133-44.
60. Wree A, Kahraman A, Gerken G, Canbay A. Obesity affects the liver - the link between adipocytes and hepatocytes. Digestion 2011;83:124-33.
61. Marra F, Bertolani C. Adipokines in liver diseases. Hepatology 2009;50:957-69.
62. Dixon LJ, Flask CA, Papouchado BG, Feldstein AE, Nagy LE. Caspase-1 as a central regulator of high fat diet-induced non-alcoholic steatohepatitis. PLoS One 2013;8:e56100.
63. Roderfeld M, Weiskirchen R, Wagner S, Berres ML, Henkel C, Grotzinger J, Gressner AM, Matern S, Roeb E. Inhibition of hepatic fibrogenesis by matrix metalloproteinase-9 mutants in mice. Faseb J 2006;20:444-54.
64. Iredale JP. Models of liver fibrosis: exploring the dynamic nature of inflammation and repair in a solid organ. J Clin Invest 2007;117:539-48.
65. Friedman SL. Mechanisms of hepatic fibrogenesis. Gastroenterology 2008;134:1655-69.
66. Guicciardi ME, Malhi H, Mott JL, Gores GJ. Apoptosis and necrosis in the liver. Compr Physiol 2013;3:977-1010.
67. Weber A, Boger R, Vick B, Urbanik T, Haybaeck J, Zoller S, Teufel A, Krammer PH, Opferman JT, Galle PR, Schuchmann M, Heikenwalder M, Schulze-Bergkamen H. Hepatocyte-specific deletion of the antiapoptotic protein myeloid cell leukemia-1 triggers proliferation and hepatocarcinogenesis in mice. Hepatology 2010;51:1226-36.
68. Pierce RH, Vail ME, Ralph L, Campbell JS, Fausto N. Bcl-2 expression inhibits liver carcinogenesis and delays the development of proliferating foci. Am J Pathol 2002;160:1555-60.
69. Qiu W, Wang X, Leibowitz B, Yang W, Zhang L, Yu J. PUMA-mediated apoptosis drives chemical hepatocarcinogenesis in mice. Hepatology 2011;54:1249-58.
70. Chen L, Park SM, Tumanov AV, Hau A, Sawada K, Feig C, Turner JR, Fu YX, Romero IL, Lengyel E, Peter ME. CD95 promotes tumour growth. Nature 2010;465:492-6.